Internal dynamics of poly(glutamic acid) arborescent polymers probed by fluorescence

Timothy Hall, Greg Whitton, Mario Gauthier, Jean Duhamel, Department of Chemistry, University of Waterloo, ON N2L 3G1, Canada

Protein folding is required to generate functional proteins whose catalytic activity is necessary for many biological processes. Extensive scientific research has been dedicated to studying many aspects of protein folding, since its understanding has a direct impact on improving human life. An important element in predicting how proteins fold involves the characterization of the internal dynamics of polypeptide chains. Fluorescence quenching experiments that rely on the attachment of a fluorescent probe to a macromolecule yield information on its internal dynamics, whether the macromolecule is flexible or rigid, present as a single unit, or aggregated. When such experiments are conducted on fluorescently labelled macromolecules that are protein analogues, they describe the time scale over which amino acids encounter as the protein analogue folds. Pyrene is an ideal probe for many fluorescence quenching studies because an excited pyrene monomer can be quenched by forming an excimer upon encounter with a ground-state pyrene monomer.[1] This process of excimer formation can be detected using steady-state and time resolved fluorescence. In this study, 1-pyrenemethylamine was covalently attached to three types of polymeric constructs, namely linear, comb-branched, and arborescent poly(L-glutamic acid) (PGA), to obtain information about their structure and internal dynamics in solution from the analysis of their fluorescence spectra and decays. PGA was selected because it adopts α-helical and random coil conformations in *N,N*-dimethylformamide (DMF) and in dimethyl sulfoxide (DMSO), respectively, while the inherently compact nature of arborescent polymers in general and arborescent PGAs in particular makes them representative mimics of globular proteins.

Experimental

Low dispersity poly(γ–benzyl L–glutamate) (PBG) was synthesized by ring opening polymerization of the corresponding *N*-carboxyanhydride derivative using a primary amine initiator.[2,3] These chains were grafted onto a linear PBG backbone using carbodiimide coupling to create a comb-branched (or arborescent generation G0) polymer with a narrow molecular weight distribution.[4] Further grafting reactions yielded arborescent polymers of generations G1–G3. The benzyl groups of PBG were removed through acidolysis to yield poly(L-glutamic acid) (PGA). 1-Pyrenemethylamine was covalently bonded to 2-15 % of the glutamic acid units via a carbodiimide coupling reaction, thereby generating samples randomly labelled with pyrene.[5]

For the steady-state and time-resolved fluorescence studies, all pyrene labelled polymer samples were dissolved in spectrophotometric-grade solvent, diluted to an absorbance of 0.1

equivalent to a 2.5×10^{-6} M pyrene concentration, before being degassed with a steady stream of nitrogen for a minimum of 35 minutes prior to carrying out the fluorescence measurement.

Steady-state fluorescence emission spectra for all the samples were obtained over the wavelength range 350-600 nm using an excitation wavelength of 344 nm. The ratio of the fluorescence intensity for the excimer over that for the monomer, the I_E/I_M ratio, was calculated for each sample.

Time-resolved fluorescence decays for the pyrene monomer and excimer were acquired by exciting the samples at 344 nm and monitoring the emission at 375 nm and 510 nm, respectively. The decays were fitted globally using the fluorescence blob model.[6]

Results

Fluorescence spectra for the pyrene-labelled samples acquired in DMF and in DMSO are shown in Figure 1 for the G3 poly(L-glutamic acid) sample (Py-G3 PGA) after normalization to the monomer peak at 375 nm. As the pyrene content increases, the excimer emission intensity centered at 480 nm increases. Less excimer is formed in DMSO than in DMF. These differences are influenced by both the internal dynamics of the macromolecules and the solvent viscosity.

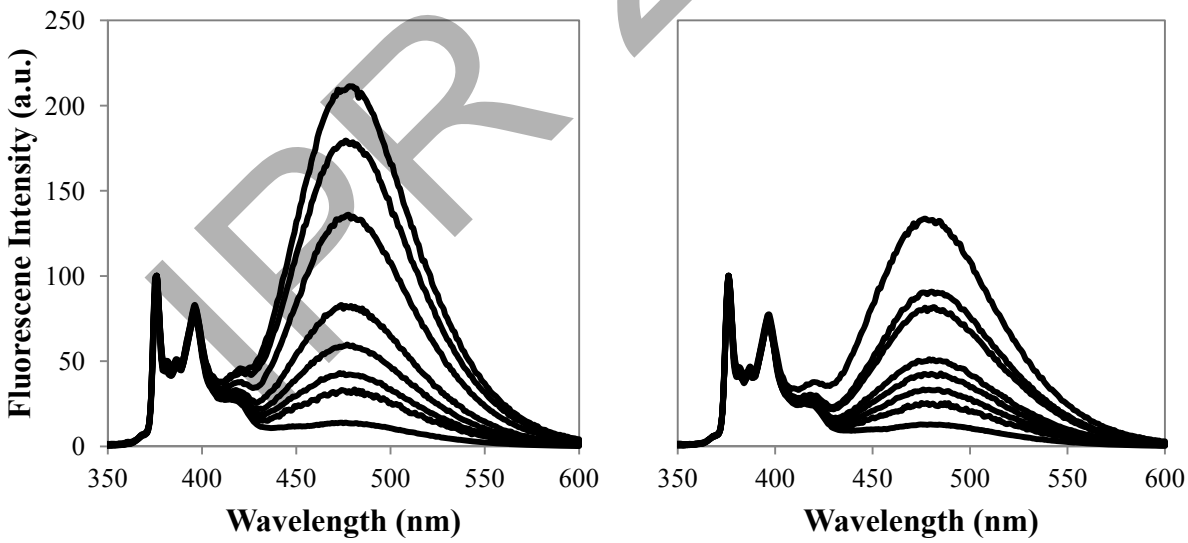

Figure 1: Steady-state fluorescence spectra of G3-Py PGA in DMF (left) and DMSO (right). The pyrene contents are 12.6, 11.4, 10.9, 9.4, 8.1, 6.6, 5.4, and 4.0 mol % from top to bottom.

To account for the different solvent viscosities of DMF (0.79 mPa·s) and DMSO (2.0 mPa·s) at 25 °C, the I_E/I_M ratios obtained from the fluorescence spectra were multiplied by the solvent viscosity. Figure 2 shows the product $\eta \times I_E/I_M$ for linear, Py-G1, and Py-G3 PGAs. For each PGA construct $\eta \times I_E/I_M$ increases with increasing pyrene content, reflecting more efficient excimer formation with increased local pyrene concentration ($[Py]_{loc}$). Furthermore, $\eta \times I_E/I_M$ for a given pyrene content increases according to the sequence G3 > G2 > G1 > G0 > linear, in agreement with the increased density and $[Py]_{loc}$ of the constructs. This trend is more pronounced in DMSO than in DMF. Finally, $\eta \times I_E/I_M$ for a given construct is larger in DMSO than in DMF, suggesting that the PGA constructs undergo faster dynamics in DMSO, possibly due to the conformation change undergone by PGA when changing from an α–helix (in DMF) to a random coil (in DMSO).

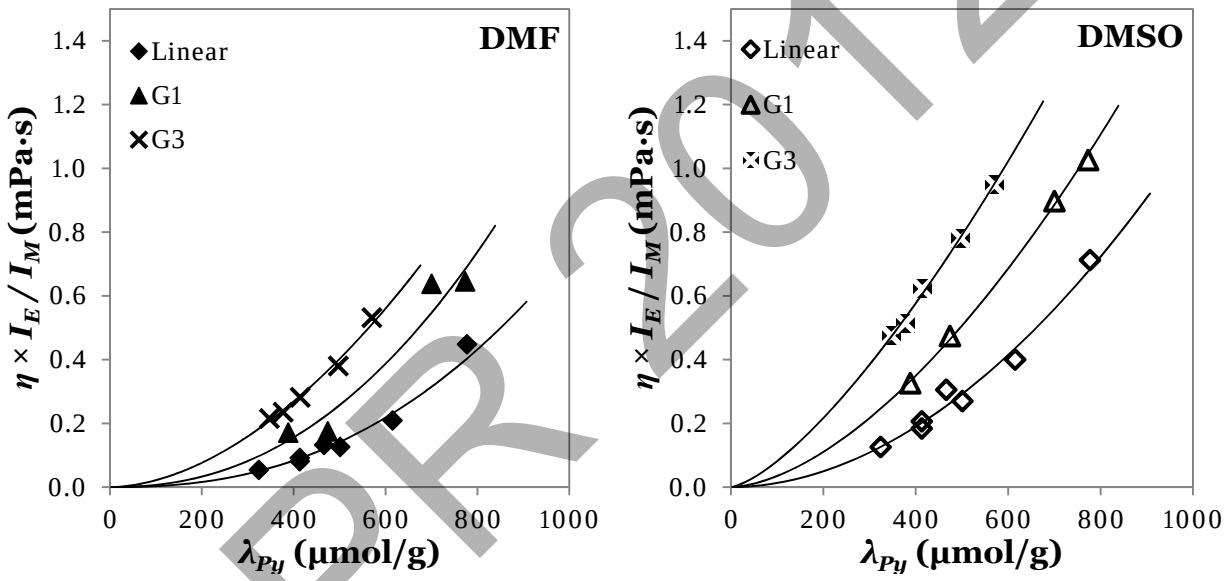

Figure 2: Plots of $\eta \times I_E/I_M$ versus pyrene content in DMF (left) and DMSO (right) for linear (diamond), Py-G1 (triangle), and Py-G3 (crosses) PGAs.

To determine the timescale over which excimer formation takes place in the pyrene-labelled PGA constructs, time-resolved fluorescence decays for the monomer and excimer species of all Py-PGA samples were acquired and fitted globally with the Fluorescence Blob Model (FBM).[6] According to the FBM, a blob is defined as the volume of space that can be probed by an excited pyrene during its lifetime, and N_{blob} is the number of structural units located inside a blob. N_{blob} was determined for all the pyrene-labelled PGA constructs in DMF and DMSO, and is shown in Figure 3 as a function of the corrected pyrene content. N_{blob} equals 14 for the linear PGA chains, a slightly smaller value than the number-average degree of polymerization of 16, which implies that the excited pyrene probes the entire PGA segment

regardless of its conformation. The N_{blob} values for PGA increase as the generation number of the PGA construct increases, implying that although pyrene excimer formation occurs intramolecularly inside a PGA construct, there are increased interactions between different PGA side-chains. It is noteworthy that larger N_{blob} values are obtained in DMSO, where PGA is expected to adopt a random coil conformation. Comparatively, the helical conformation induced by DMF leads to PGA segments that are more rigid, with fewer interactions between branches.

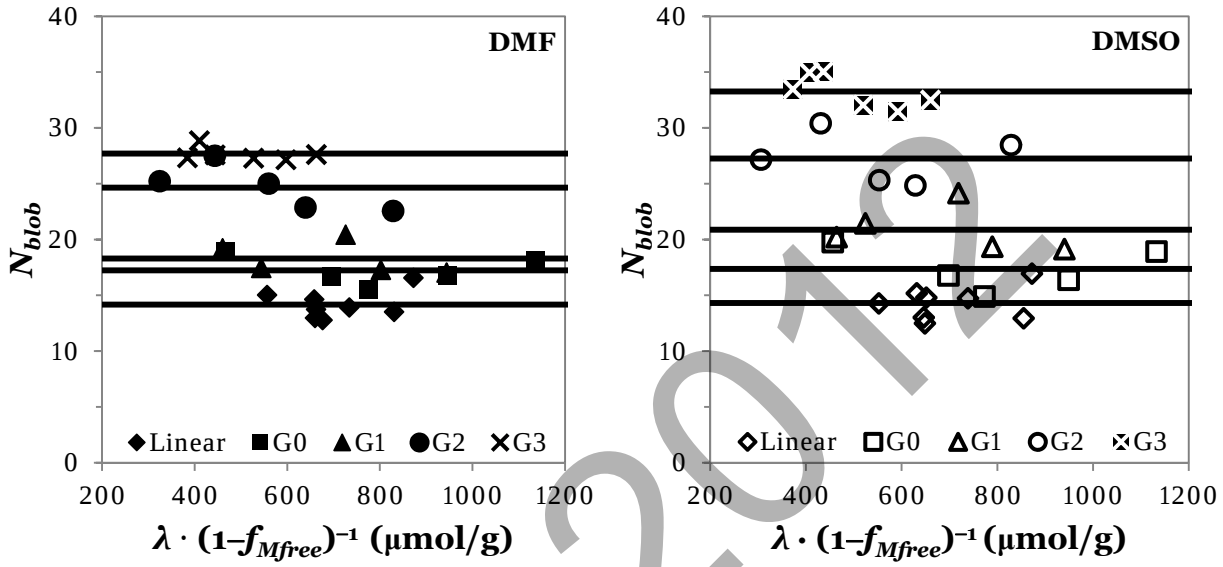

Figure 3: Plots of N_{blob} versus corrected pyrene content for linear (diamond), Py-G0 (square), Py-G1 (triangle), Py-G2 (circles), and Py-G3 (crosses) PGA constructs in DMF (filled) and DMSO (hollow).

In addition to providing information on polymer coil density, FBM analysis of the fluorescence decays can also be used to describe the dynamics of the side-chains. For polymers randomly labelled with pyrene, k_{blob} is retrieved from the FBM analysis of the fluorescence decays. It represents the rate constant of excimer formation between one excited pyrene and one ground-state pyrene located inside a blob. The product $k_{blob} \times N_{blob} \times \eta$ (where η is the solvent viscosity) has been shown to describe the internal dynamics of a macromolecule randomly labelled with pyrene. The product $k_{blob} \times N_{blob} \times \eta$ was plotted as a function of pyrene content for each PGA construct in Figure 4. In each solvent, a general trend is obtained where $k_{blob} \times N_{blob} \times \eta$ increases with increasing generation number, reflecting the larger $[Py]_{\text{loc}}$ generated in the more compact PGA constructs. Also, the PGA constructs in DMSO appear to undergo much more rapid pyrene excimer formation, possibly due to the random coil conformation adopted by the PGA chains in DMSO.

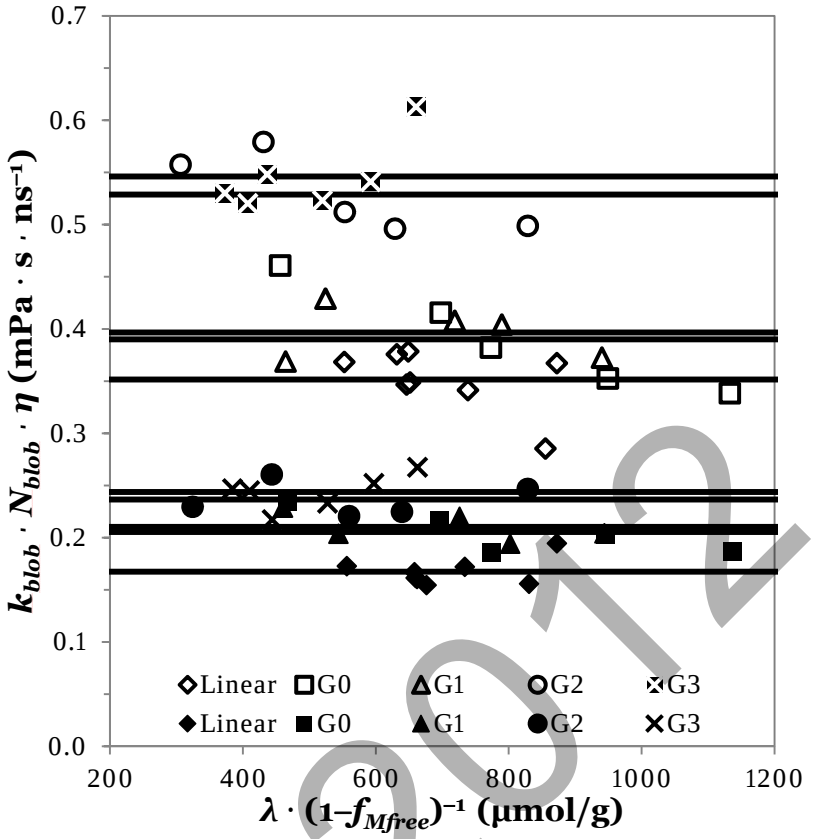

Figure 4: Plots of $k_{blob} \times N_{blob} \times \eta$ versus corrected pyrene content showing the differences in internal dynamics for linear (diamond), Py-G0 (square), Py-G1 (triangle), Py-G2 (circles), and Py-G3 (crosses) PGA constructs in DMF (filled) and DMSO (hollow).

Conclusions

This study represents the first example in the scientific literature of an investigation of the internal dynamics of a series of protein analogues by fluorescence. It demonstrates that the helix-to-coil transition experienced by the PGA building blocks has a strong effect on the dynamics inside the macromolecule.

References

1. Duhamel, J. ASAP *Langmuir* **2012**.
2. Doty, P.; Bradbury, J. H.; Holtzer, A. M. *J. Am. Chem. Soc.* **1956**, *78*, 947–954.
3. Mitchell, J. C.; Woodward, A. E.; Doty, P. *J. Am. Chem. Soc.* **1957**, *79*, 3955–3960.
4. Whitton, G.; Gauthier M.; *Thirty-First Annual Symposium on Polymer Science/Engineering Documents* **2009**.
5. Duhamel, J.; Kanagalingam, S.; O'Brien, T. J.; Ingratta, M. W. *J. Am. Chem. Soc.* **2003**, *125*, 12810–12822.
6. Mathew, A.; Siu, H.; Duhamel, J. *Macromolecules* **1999**, *32*, 7100-7108.

Probing the Internal Dynamics of Poly(L-Glutamic Acid)

May 2, 2012
IPR Symposium

Timothy Hall
Greg Whitton
Mario Gauthier
Jean Duhamel

1

Future of Medicine

- Proteomics
  - Study of protein structure, function, and folding
  - Providing targets for drug development
  - Study of protein's role in diseases such as cystic fibrosis and Alzheimer
- Predicting the protein folding pathway
  - Characterization of the internal dynamics of polypeptide chains

2

Protein Folding

1) Random coil

2) Hydrophobic collapse

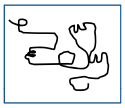

3) Secondary structure

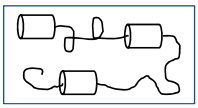

4) Folded Protein

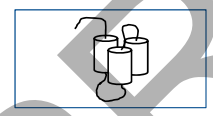

3

Pyrene

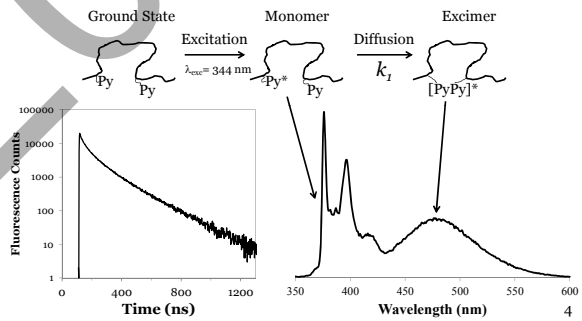

4

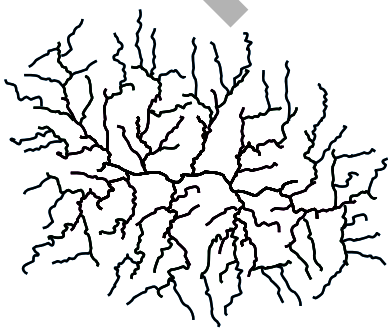

Arborescent Polymer

5

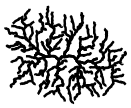

SIZE	R_h=	2 – 10 nm	5 – 15 nm
	M_n=	1.67×10^4 – 3.00×10^5 g·mol^{-1}	3.30×10^4 – 6.54×10^5 g·mol^{-1}
AMINO ACIDS		All 20	Glutamic Acid
SECONDARY STRUCTURE		Random Coil α-helix β-sheets	Random Coil α-helix

6

Poly(γ-benzyl L-glutamate)

Generation	Macromolecule M_n^{GPC} (g·mol^{-1})	Macromolecule $\frac{M_w}{M_n}$	Side-chains M_n^{NMR} (g·mol^{-1})	Side-chains DP_n	Branching functionality
Linear[a]	3.60×10^3	1.09	-	-	-
G0	5.30×10^4	1.04	6600	30	6.6
G1	1.33×10^5	1.06	4000	18	28
G2	4.86×10^5	1.03	3900	17	124
G3	1.06×10^6	1.03	3900	17	289

[a] M_n calculated using a DP_n of 16 determined from ^{1}H NMR.

Samples provided by Greg Whitton

7

Poly(L-glutamic acid)

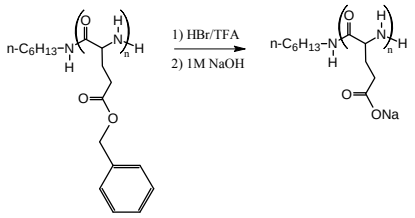

Poly(γ-benzyl L-glutamate)
PBG

Poly(L-glutamate)
Poly(L-glutamic acid)
PGNa/PGA

Arborescent samples provided by Greg Whitton

8

^{1}H NMR Peak Assignments

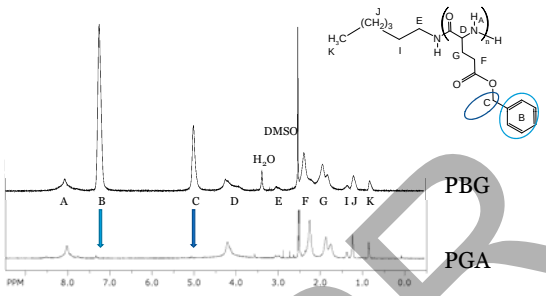

PBG

PGA

9

Chain conformations of PGA/PBG

α-Helix

Random Coil

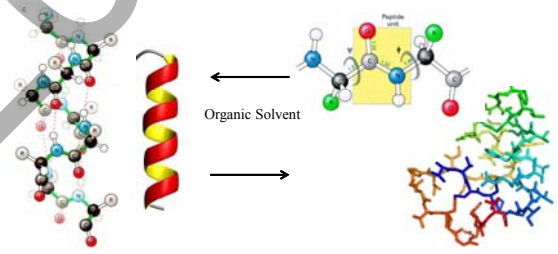

Organic Solvent

DMF

DMSO

10

^{1}H NMR G2 PGA

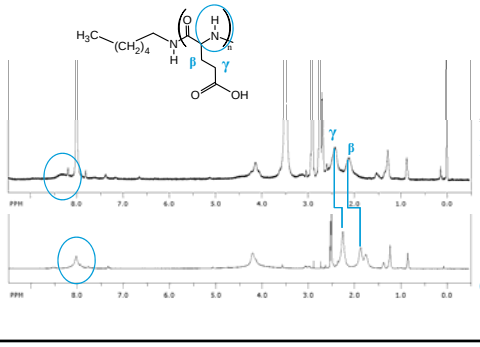

Helical
DMF

DMSO
Coil

^{1}H NMR G1 PGA

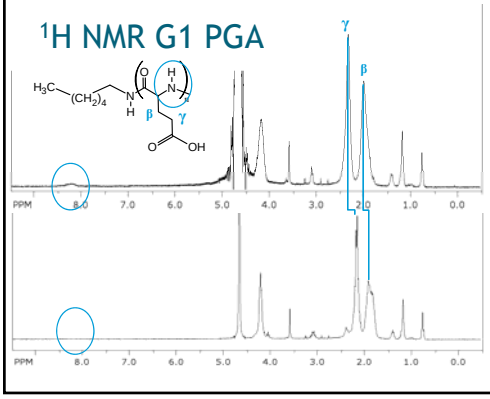

Helical
D_2O/HCl
pH 5

Coil
D_2O pH 8

2

DLS: Hydrodynamic size

10 mg/mL sample concentration

0.5 mg LiBr /mL added to suppress aggregation

Generation	Diameter	
	DMF	DMSO
G1	11.0	16.4
G2	15.4	20.7
G3	31.2	30.3

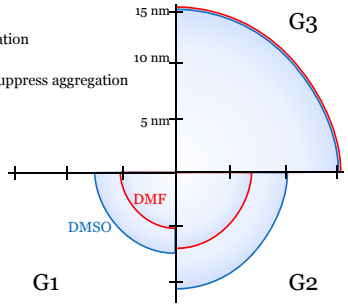

13

Fluorescence Studies

14

Polymer Labeling

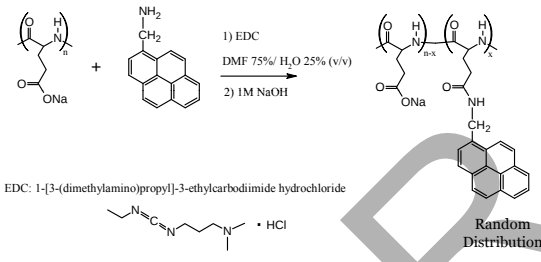

EDC: 1-[3-(dimethylamino)propyl]-3-ethylcarbodiimide hydrochloride

Ingratta *et al. J. Am. Chem. Soc.* **2003**, *125*, 12810-12822.

15

GPC Fluorescence Detector

Purification by liquid-liquid extraction and dialysis

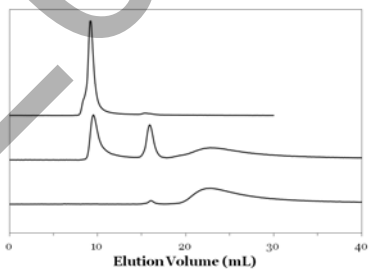

Py-PGA Linear

Impure sample

1-Pyrenemethylamine

DMF

λ_{exc}= 344 nm

λ_{emm}= 375 nm

16

Py-G3 PGA Emission

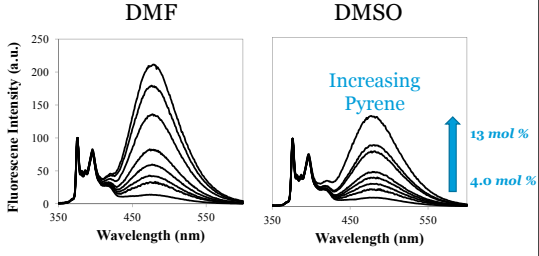

λ_{exc}= 344 nm

17

I_E / I_M

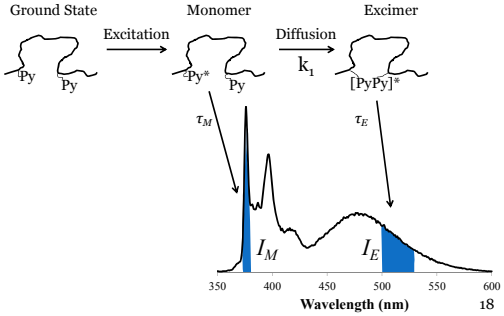

18

Py-PGA Excimer Formation

DMF DMSO

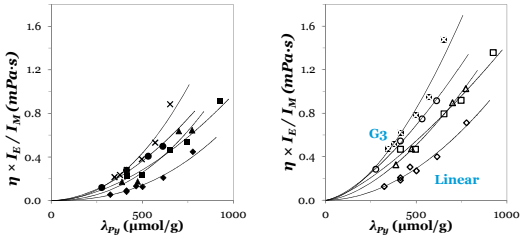

linear (◆,◇), Py-Go (■,□), Py-G1 (▲,△), Py-G2 (●,○), and Py-G3 (✕, ⊠)

19

Py-G3 PGA Decays in DMF

Monomer Excimer

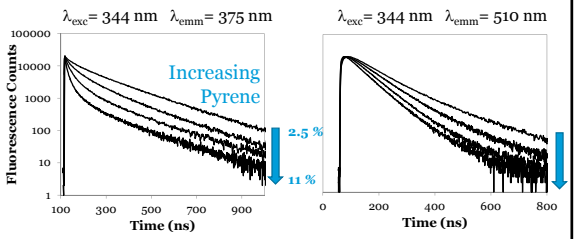

20

Decay Analysis

- Fluorescence Blob Model
  - Accounts for the distribution of rate constants
  - Describes the time scale of excimer formation and average pyrene spacing

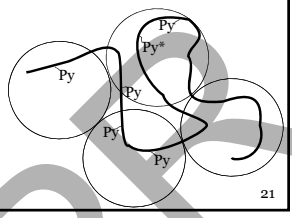

21

Excimer Formation

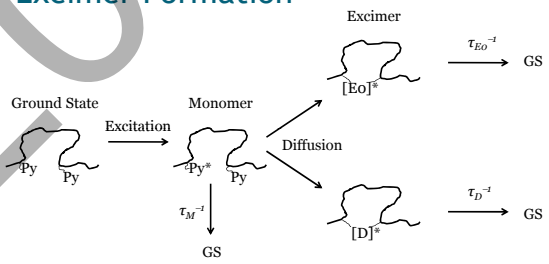

Model also takes into account direct excitation of pre-associated pyrene (without chain diffusion or pyrene rearrangement)

22

FBM Parameters

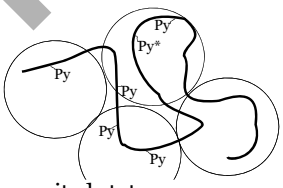

- *Blob* - Volume probed by excited state pyrene
- Lifetimes: τ_M, τ_{Eo}, τ_D
- Rate constants: k_2, k_{blob}, k_{exch}
- N_{blob} - Number of structural units within a blob
- $k_{blob} \times N_{blob} \times \eta$ – Measure of the internal dynamics of the macromolecules

23

FBM Analysis

Fixed Values	DMF	DMSO
τ_M (ns)	210 ± 2	170 ± 1
τ_D (ns)	70± 8	70 ± 9
k_2 (ns^{-1})	0.17 ± 0.05	0.12 ± 0.03

- Monomer lifetimes determined experimentally
- Excimer lifetimes and k_2 were optimized in the analysis
- Subsequent analysis used average values for τ_D and k_2

24

FBM: N_{blob}

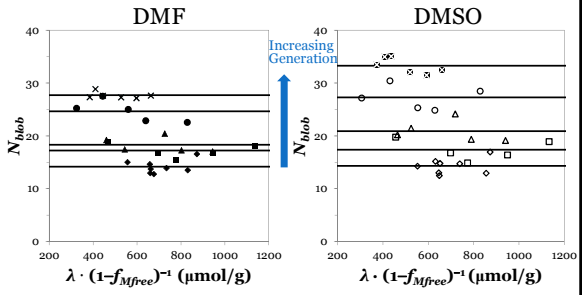

linear (◆,◇), Py-Go (■,□), Py-G1 (▲,△), Py-G2 (●,○), and Py-G3 (✕, ⊠)

25

FBM: $k_{blob} \cdot N_{blob} \cdot \eta$

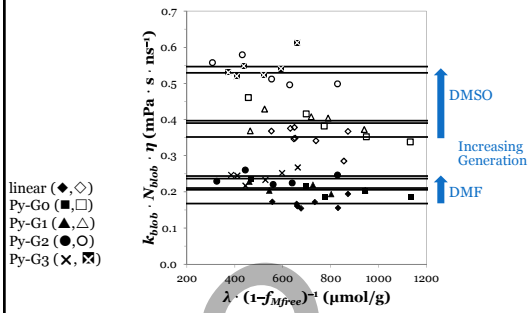

26

FBM: Study Summary

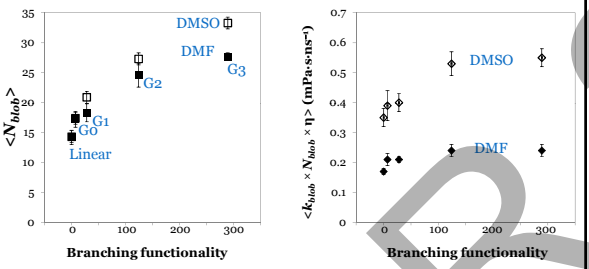

27

Summary

- Analysis indicates that the dynamics are faster for side chain interactions in DMSO than in DMF
- The helical segments of dendrigraft PGA are rigid in DMF, with fewer interactions than in DMSO

28

Future Studies

- Vary the composition of the Py-PGA side chains, incorporating labelled and unlabelled branches during the dendrigraft synthesis
- Study the internal dynamics of additional polypeptides

29

Acknowledgements

- Gauthier & Duhamel Lab Colleagues
- Nathan Julius (Nate) Grishkewich & Tam Lab
- Jan Venne, NMR Watspec

IPR NSERC CRSNG Waterloo Department of Chemistry Graduate Studies Office

30